

## CHAPTER IV

### RESULTS AND DISCUSSION

#### 4.1 Determination of Conditions for Measurement of Intrinsic Rate Constants

In order to evaluate intrinsic rate constants, it is necessary to minimize and, if possible, to eliminate mass transfer resistance effects. In this work, conditions where mass transfer effects can be considered negligible were determined empirically. First, a series of runs were done at different feed rates, but at the same W/F ratio (W is the weight of catalyst and F is the gas flowrate (g/h)). Conversion is determined in the region where external mass transfer resistance is not significant. Second, a series of runs were performed with different catalyst sizes,  $d_p$ , but at the same value of W/F ratio in order to define the region where intraparticle mass transfer resistance can be neglected.

##### 4.1.1 Study of a Limitation in External Transfer

The search for conditions where hydrogenation of tetralin is not controlled by external mass transfer resistance was done through a series of experiments illustrated in Figure 4.1. On these experiments a constant hydrogen flowrate of 250 mL/min was fixed while the flowrate of liquid was varied. From Figure 4.1, it can be seen that for a liquid flowrate equal or greater than 3.66 mL/min mass transfer resistance is not the controlling step.

##### 4.1.2 Study of a Limitation in Internal Transfer

To determine the region where internal mass transfer resistance does not limit the conversion, the diameter of the catalyst pellet was varied. The flowrate of Hydrogen was 250 mL/min and the liquid flowrate was 3.66 mL/h. The results are shown in Figure 4.2. It is clear from Figure 4.2 that for diameters of particle lower than approximately 0.32 mm the internal mass transfer resistance is negligible.

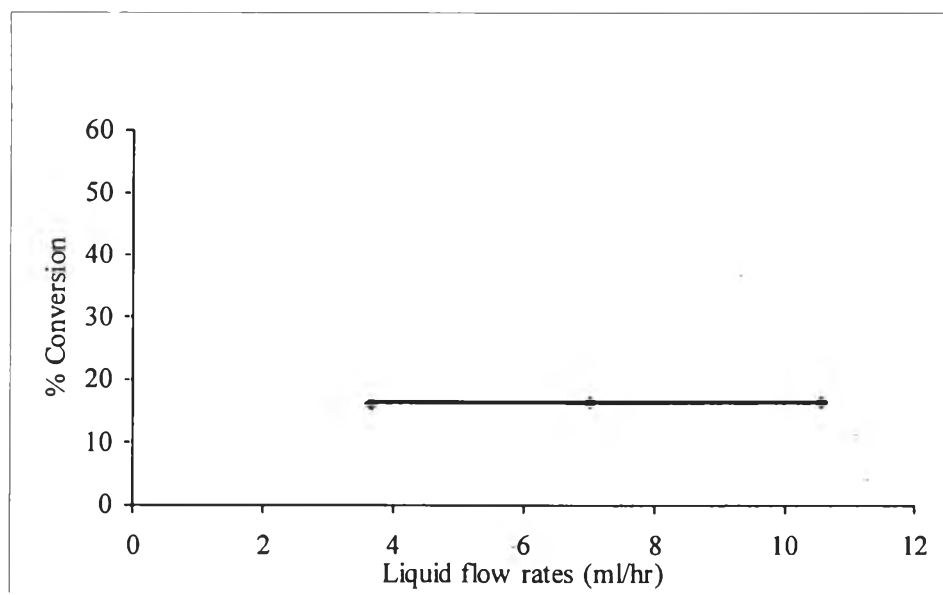


**Figure 4.1** Test for the external transfer resistance at 300 psig and 300°C by varying liquid flowrate.

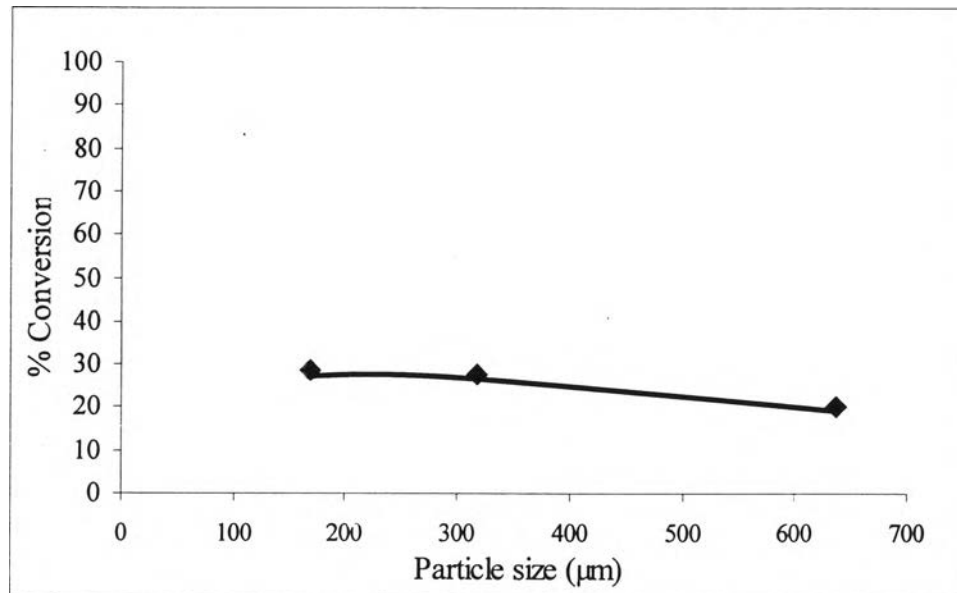


**Figure 4.2** Test for the internal transfer resistance at 300 psig and 300°C by varying particle sizes.

## 4.2 Hydrogenation Results

The hydrogenation of tetralin was carried out at temperatures of 255-300 °C, constant total pressure of 300 psi and constant hydrogen/hydrocarbon molar feed ratio of 25. Under these conditions, only two main products which are *trans*- and *cis*- decalin were found. Although the hydrogenation of aromatic compounds are generally considered as the reversible reactions (Sapre and Gates, 1981), but the small amounts of dehydrogenation product, naphthalene, was found over all the conditions of this study. Therefore the dehydrogenation reaction could be neglected. Based on the reaction products, tetralin hydrogenation can be described by these three reactions:



These reactions were also proposed by Weikamp (1968). The first two reactions are the hydrogenation of tetralin to *cis*- and *trans*- decalin respectively. Due to the high total pressure and hydrogen/hydrocarbon molar feed ratio, the hydrogenations of tetralin are considered irreversible. The last reaction is the reversible isomerization of *cis*- and *trans*- decalin. This reaction was taken place at high conversion of tetralin (Jongpatiwut *et al.*, 2004).

### 4.2.1 *Trans*- to *Cis*- Decalin Ratio

The *trans*/*cis* ratio in the decalin product as a function of tetralin conversion was observed on the different temperatures. As shown in Figure 4.3 the *trans*/*cis* ratios are independent of temperatures, but it can be seen that *trans*/*cis* ratio slightly increased with tetralin conversion. This is caused by the *trans*/*cis* isomerization are increased when the tetralin decreased. Huang and Kang (1995) proposed that the *trans*/*cis* isomerization is inhibited by the presence of tetralin. This

is also similar to the hydrogenation of tetralin over supported Pt and Pd in which the trans/cis isomerization is occurred at the conversion of tetralin more than 70% (Jongpatiwut *et al.*, 2004).

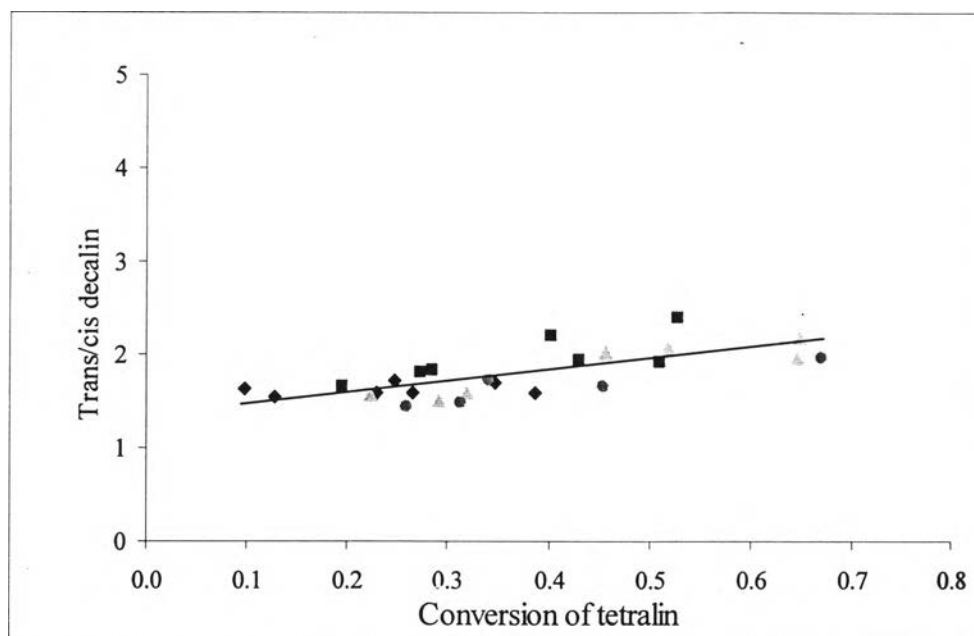


**Figure 4.3** *Trans-/cis-*decalin ratios in the product of tetralin hydrogenation as a function of tetralin conversion at different temperatures. Diamonds, squares, triangles, and cycles represent data at the temperature of 300, 285, 270 and 255 °C, respectively.

#### 4.2.2 Effect of Temperature

The observed conversions as a function of the temperatures are shown in Figure 4.4. As can be seen in this figure, the conversions decreased with an increasing temperature throughout the W/F of this study. This behavior is not caused by thermodynamic limitations because the equilibrium conversion of tetralin is above 95% at 300 °C and 100% at the temperature below 290 °C. The equilibrium conversion of tetralin was obtained by HSC 5.0 program. The high equilibrium conversion is due to the high hydrogen to tetralin molar feed ratio (25 times) and high total pressure. Therefore, the decreased conversion with increasing temperature can be explained by the increasing of the hydrogenation rate constant with the

temperature is overcompensated by the decreasing of adsorption constant included in the rate expression. In addition, the surface coverage of the reaction intermediate in the rate determining step is decreased at higher temperatures. Moreover, at higher temperature the sites required for adsorbed hydrogen are decreased which cause the adsorption capacity of hydrogen decreased. This phenomenon was explained by the study of hydrogen chemisorption on Ni catalyst (Smed *et al.*, 1996). The decreasing of hydrogenation rates at higher temperature were frequently found in the gas phase hydrogenation of aromatics (Smeds *et al.*, 1996, and Lindfors and Salmi, 1993).

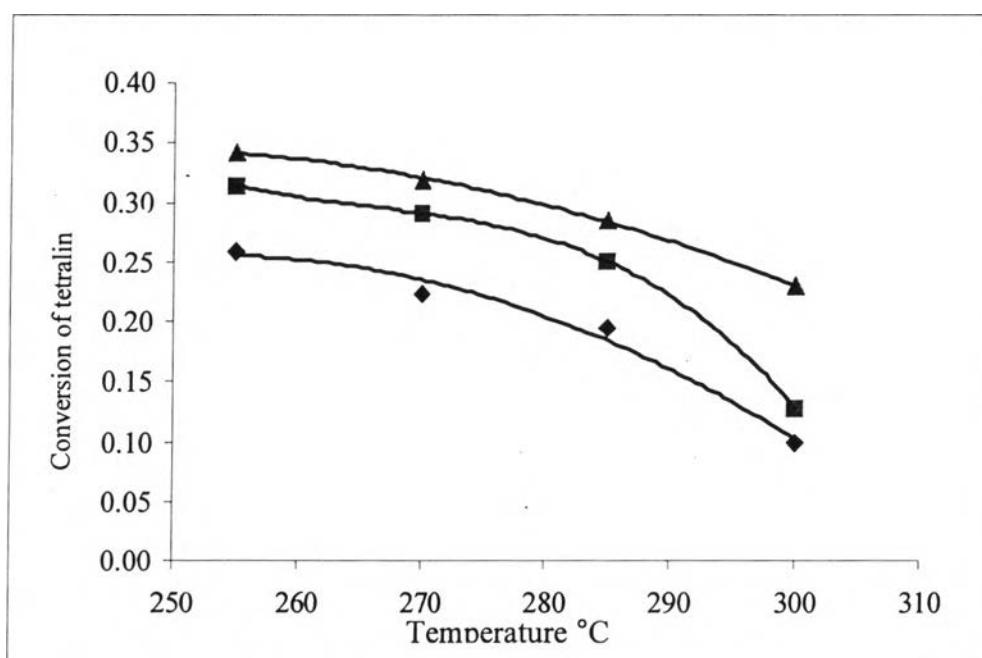


**Figure 4.4** The tetralin conversion as the function of temperatures at different W/F ratios. Triangles, squares and diamonds represent W/F of 0.011, 0.009 and 0.006 hr, respectively.

### 4.3 Kinetic Models

The most significant result of this study is the finding that only one model could successfully fit the tetralin hydrogenation data at all temperatures and also provide physically meaningful parameter. According to the proposed reactions (Eqs 4.1-4.3), the generalized Langmuir-Hinshelwood model which is usually used for the

aromatics hydrogenation can be expressed as follows (Rautanen *et al.*, 2001 and Korre *et al.*, 1995):

$$r_1 = \frac{k_1 K_T K_{H_2} P_T^{n_1} P_{H_2}^{n_2}}{(1 + K_T P_T + K_{CD} P_{CD} + K_{TD} P_{TD} + \sqrt{K_{H_2} P_{H_2}})^2} \quad (4.4)$$

$$r_2 = \frac{k_2 K_T K_{H_2} P_T^{n_1} P_{H_2}^{n_2}}{(1 + K_T P_T + K_{CD} P_{CD} + K_{TD} P_{TD} + \sqrt{K_{H_2} P_{H_2}})^2} \quad (4.5)$$

$$r_3 = \frac{k_3 K_{CD} (P_{CD} - \frac{P_{CD}}{K_{CD-TD}})}{(1 + K_T P_T + K_{CD} P_{CD} + K_{TD} P_{TD} + \sqrt{K_{H_2} P_{H_2}})^2} \quad (4.6)$$

where  $k_i$  is the rate constant of reaction  $i$  and  $K_j$  is the equilibrium adsorption constant of the substance  $j$ .

The temperature dependency of the rate constants ( $k_i$ ) and the adsorption equilibrium constants ( $K_j$ ) were described by Arrhenius's law as follows:

$$k_i = k_0 \exp\left(\frac{-E_a}{RT}\right) \quad (4.10)$$

$$K_j = \exp\left(\frac{\Delta S_j^0}{R}\right) \exp\left(\frac{-\Delta H_j^0}{RT}\right) \quad (4.11)$$

where  $E_a$  is the activation energy (J/mol),  $\Delta S_j$  is the entropy change (J/mol K) and  $\Delta H_j$  is the enthalpy (J/mol).

#### 4.3.1 Parameter Estimation

The reactor was modeled as an isothermal plug flow reactor. Due to the wide range of conversions over this study, the integral method of rate analysis was used. The reaction rates were obtained as the Eq (4.12).

$$r_i = \frac{dX_i}{d(W/F)} \quad (4.12)$$

where  $X_i$  and  $r_i$  are the conversion and the rates of species  $i$  respectively.

Parameter estimation was performed by minimizing the sum of the squares of the errors between the calculated and observed mole fractions of tetralin, *cis*-decalin and *trans*-decalin at the end of the reactor of each observation point.

$$err^2 = \sum (y_{i,cal} - y_{i,obs})^2 \quad (4.13)$$

Eq. (4.13) was minimized with the Newton's method. The nonlinear parameters of model were estimated using the Levenberg-Marquardt algorithm. The kinetic parameters at all temperatures were estimated simultaneously.

The fitting parameters were limited by physical-chemical constrains. The activation energies were forced to be positive whereas the heats of adsorption were forced to be negative for the exothermic reaction. Also, the entropy values were limited within the range established by the Boudart's criterion as shown below (Boudart, 1972):

$$41.87 \leq -\Delta S_i \leq 51.08 - (1.4 \times 10^{-3} * \Delta H_i)$$

where  $\Delta H_i$  is expressed in J/mol and  $-\Delta S_i$  in J/mol\*K.

The exponent in the adsorption term ( $Z$ ) was varied from 1-3, while the reaction order of tetralin was varied from 0 to 2. The reaction order with respect to hydrogen was not addressed explicitly because the concentration of  $H_2$  under the conditions of the study was fairly constant throughout the catalyst bed.

#### 4.3.2 Kinetic Parameters

From the fitting of the model, the kinetic parameters are summarized in Table 4.1. The reaction order with respect to the tetralin ( $n_1$ ) and hydrogen ( $n_2$ ) are equal to 1 and 0 respectively, which is usually reported for hydrogenation reaction under the excess of hydrogen (Koussathana *et al.*, 1991). The exponent in adsorption term ( $Z$ ) is equal to 2. As can be seen in Figures 4.5-4.8, it is clear that this model is able to describe the data at all temperatures.

Table 4.1 Kinetic parameters

Parameter	Value			
	255 °C	270 °C	285 °C	300 °C
$k_1$ (mol/gcat*h)	2.48	3.13	3.90	4.80
$k_2$ (mol/gcat*h)	4.57	5.91	7.54	9.49
$k_3$ (mol/gcat*h)	4.74	5.38	6.06	6.78
$K_{TL}$ (1/atm)	1.52	0.92	0.57	0.36
$K_H$ (1/atm)	23.78	11.93	6.21	3.34
$K_{CD}$ (1/atm)	0.06	0.04	0.03	0.02
$K_{TD}$ (1/atm)	0.81	0.58	0.43	0.32
$K_{CD-TD}$	14.23	13.08	12.08	11.20
Sum of $err^2$	3.38E-05	3.53E-05	4.02E-05	2.61E-05
Total $err^2$	1.35E-04			

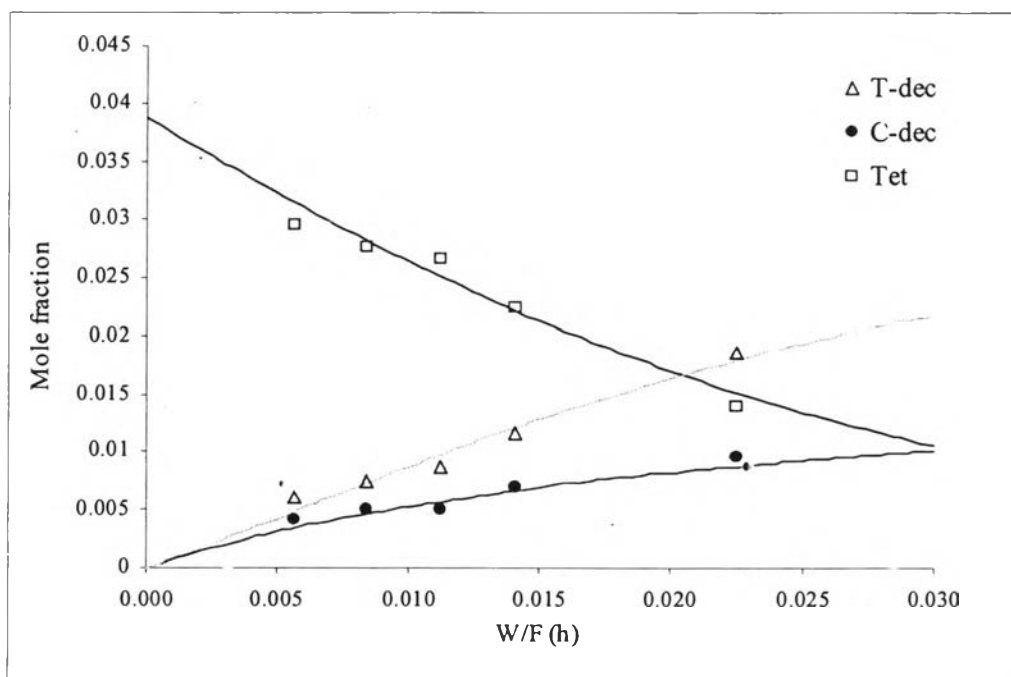
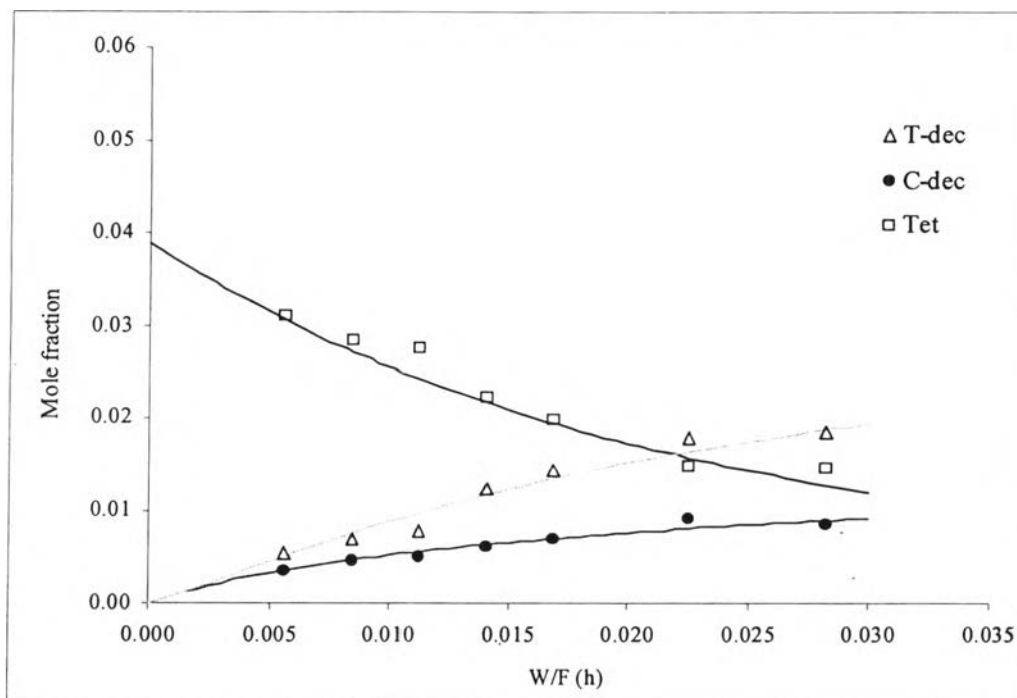
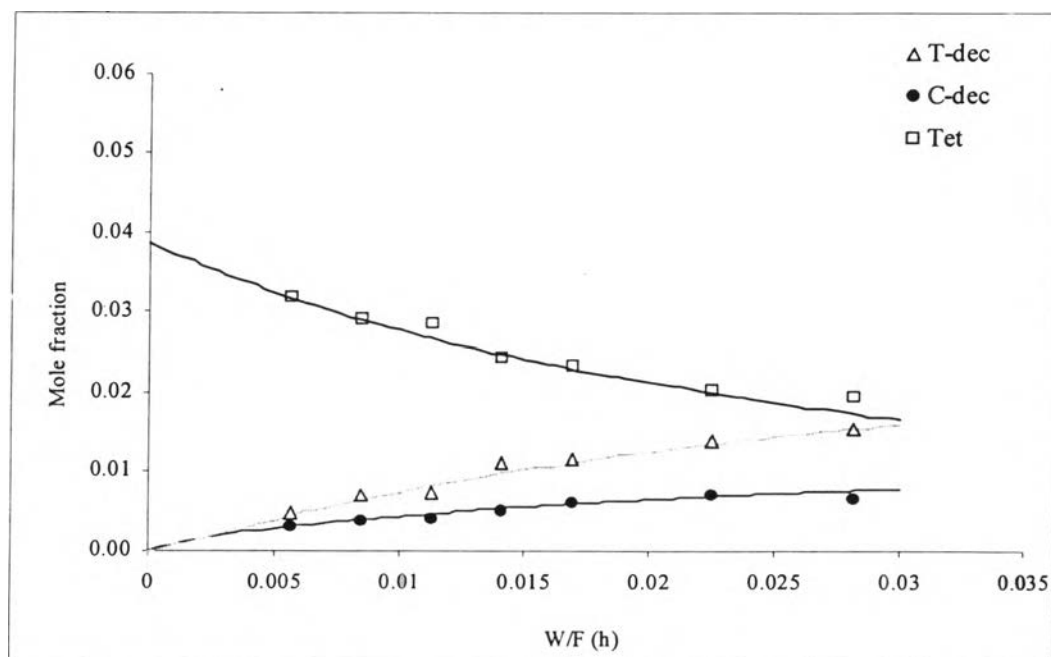


Figure 4.5 Product distributions for hydrogenation of tetralin at 255 °C. Solid lines are the values predicted by the model. Triangles, cycles and squares represent experimental mole fraction of *trans*-decalin, *cis*-decalin and tetralin, respectively.





**Figure 4.6** Product distributions for hydrogenation of tetralin at 270 °C. Solid lines are the values predicted by the model. Triangles, cycles and squares represent experimental mole fraction of *trans*-decalin, *cis*-decalin and tetralin, respectively.



**Figure 4.7** Product distributions for hydrogenation of tetralin at 285 °C. Solid lines are the values predicted by the model. Triangles, cycles and squares represent experimental mole fraction of *trans*-decalin, *cis*-decalin and tetralin, respectively.

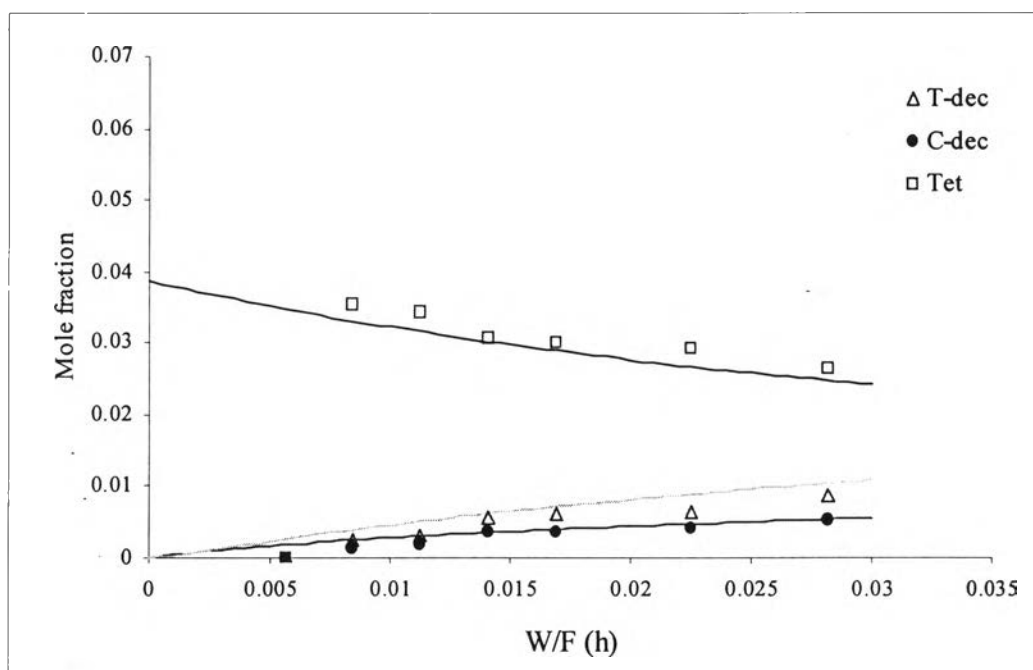


**Figure 4.8** Product distributions for hydrogenation of tetralin at 300 °C. Solid lines are the values predicted by the model. Triangles, cycles and squares represent experimental mole fraction of *trans*-decalin, *cis*-decalin and tetralin, respectively.

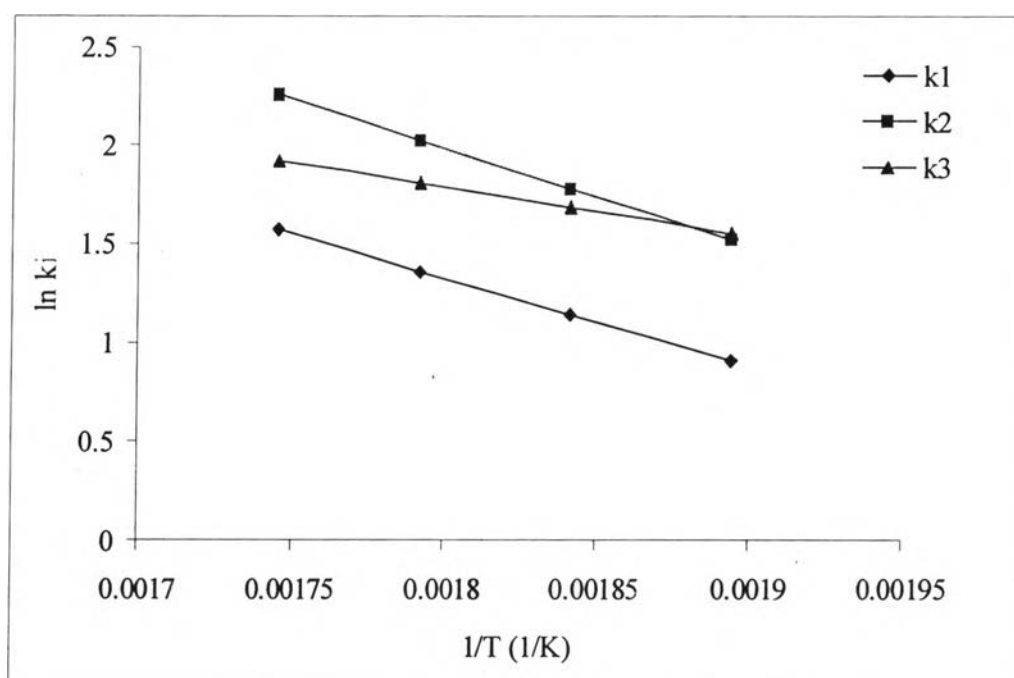
The rate constants (pre-exponential factors and activation energies) of three reactions and adsorption parameters are summarized in Tables 4.2 and 4.3. The perfectly linear behavior is observed for all the rate constants and adsorption constants as shown in Figures 4.9 and 4.10.

**Table 4.2** Rate constants

Reaction	Pre-exponential term (mol/gcat*hr)	$E_a$ (kJ/mol)
1	3.50	36.92
2	6.69	40.86
3	5.71	20.03

**Table 4.3** Heat and entropy change of adsorption

Compounds	Heat of adsorption (kJ/mol)	Entropy change (J/mol*K)
Tetralin	-80.00	-148.02
Cis-decalin	-55.87	-129.30
Trans-decalin	-51.44	-99.20
Hydrogen	-109.68	-181.38

**Figure 4.9** Arrhenius plot for the rate constants.

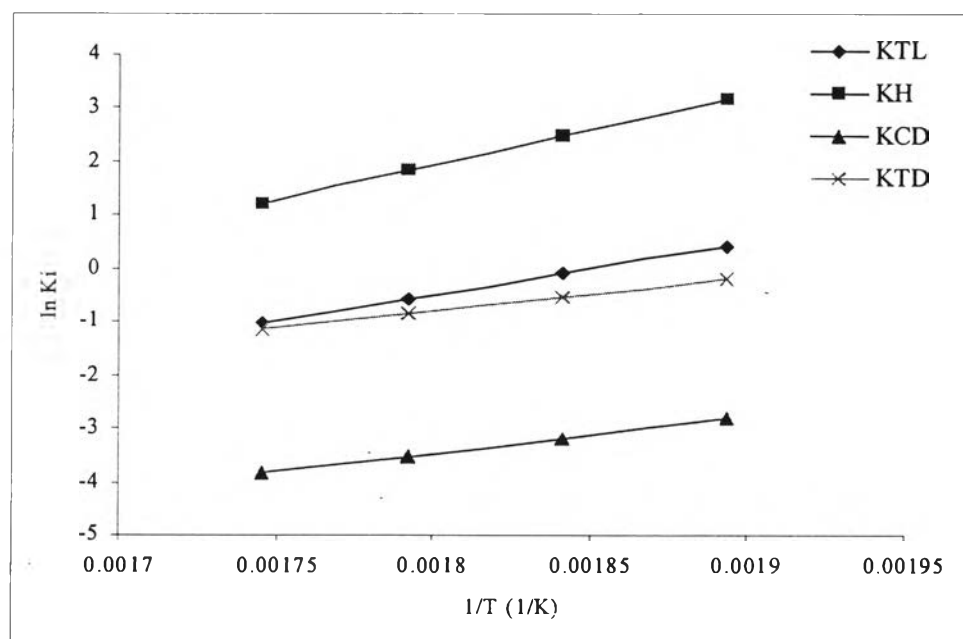


**Figure 4.10** Variation with temperature of equilibrium adsorption constants.

As can be seen in Table 4.2, the higher activation energies of hydrogenation of tetralin to *trans*-decalin compared to hydrogenation of tetralin to *cis*-decalin was found. This could be related to the more complicated reaction path that is required to produce *trans*-decalin compared to *cis*-decalin (Weitkamp, 1968). Interestingly, the reaction with the lowest activation energy is the isomerization of *cis*- to *trans*-decalin. However, the rates of this reaction are very small compare to the reaction 1 and 2. This is caused by the competitive adsorption between the aromatics. As shown in Table 4.3, heat of adsorption of *cis*-decalin is lower than tetralin. Therefore, *cis*-decalin can not overcome the other for adsorption to the site. As shown in Figures 4.11-4.14 the site coverage of *cis*-decalin is much lower than the site coverage of tetralin. The lowest surface coverage of *cis*-decalin can explain the rate of isomerization of *cis*- to *trans*-decalin is very small compare to other reactions. The rates of reaction are shown in Figures 4.15-4.18, the rate of isomerization is lower than the rate of hydrogenation at all temperatures.

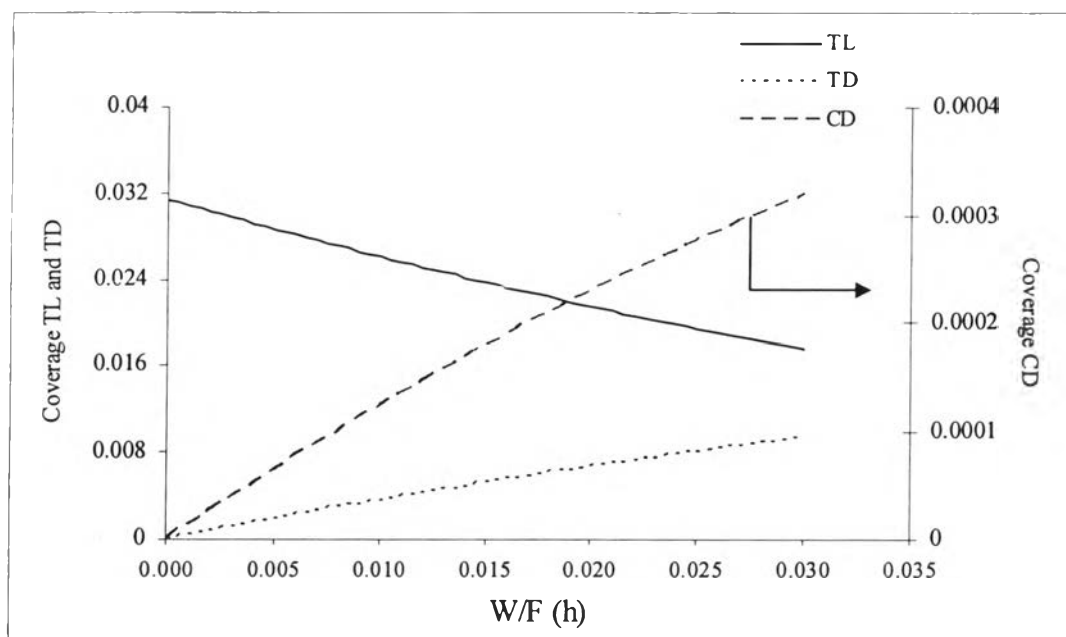


**Figure 4.11** Predicted coverage for tetralin (TL), *cis*-decalin (CD) and *trans*-decalin (TD) as a function of space time at 300 °C.

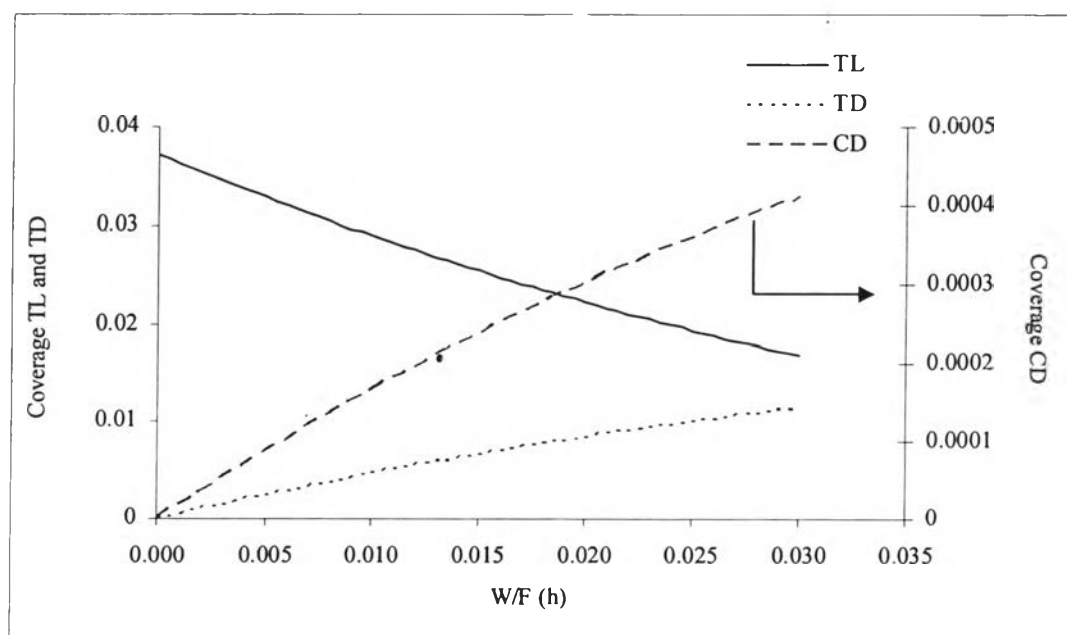


**Figure 4.12** Predicted coverage for tetralin (TL), *cis*-decalin (CD) and *trans*-decalin (TD) as a function of space time at 285 °C.

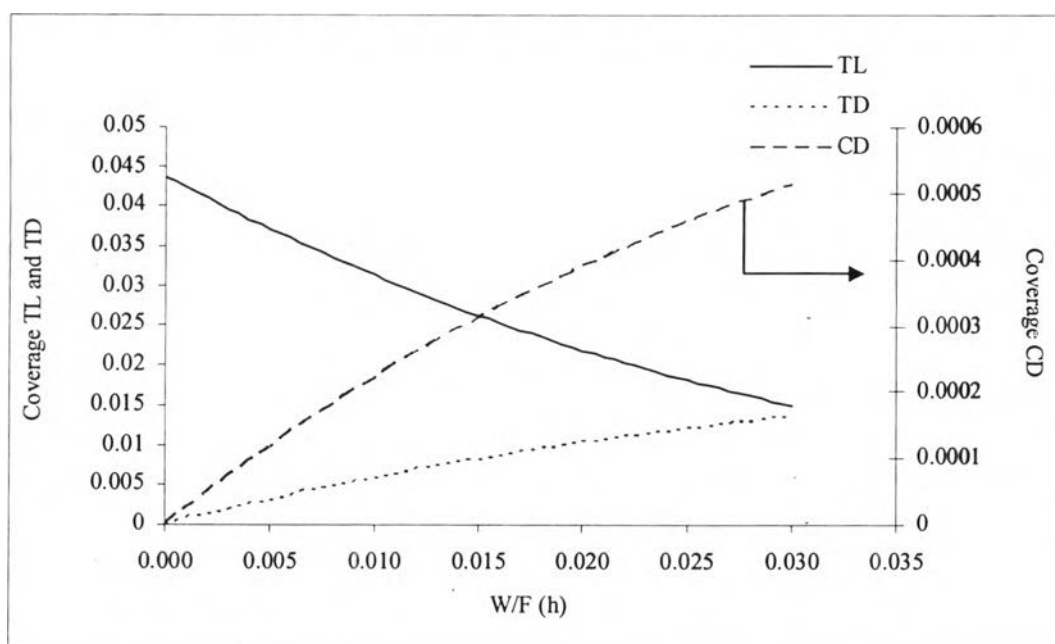


**Figure 4.13** Predicted coverage for tetralin (TL), *cis*-decalin (CD) and *trans*-decalin (TD) as a function of space time at 270 °C.

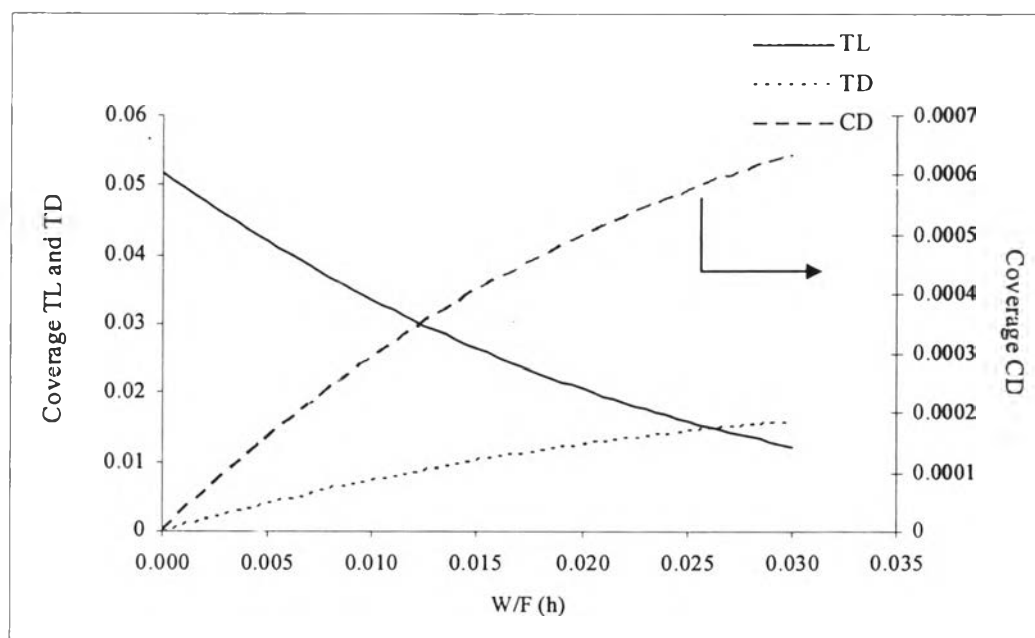


**Figure 4.14** Predicted coverage for tetralin (TL), *cis*-decalin (CD) and *trans*-decalin (TD) as a function of space time at 255 °C.

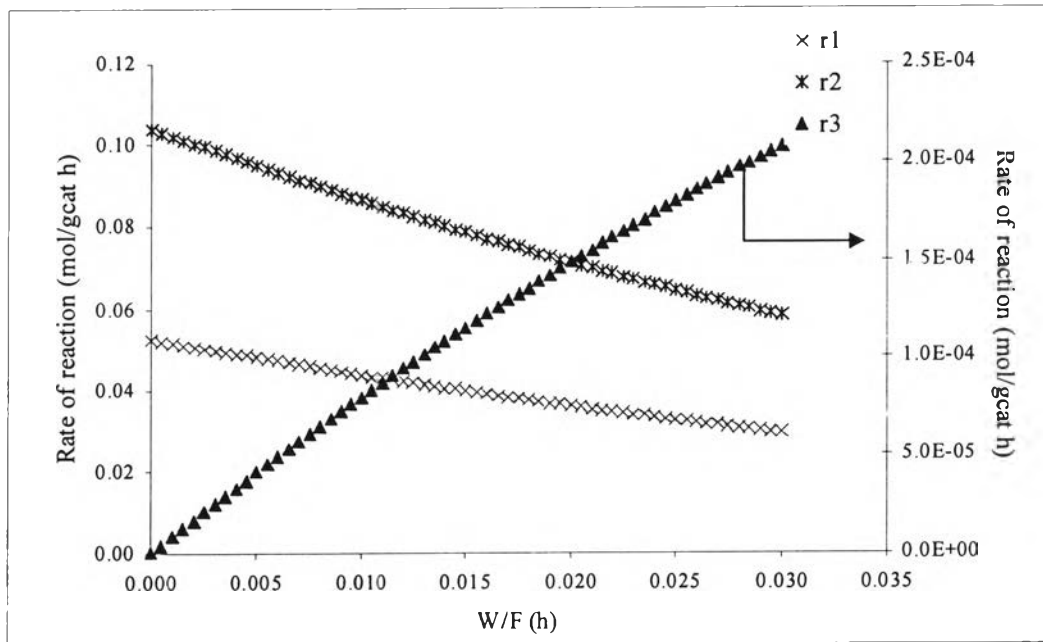


Figure 4.15 Rates of the individual reactions as a function of space times at 300 °C.

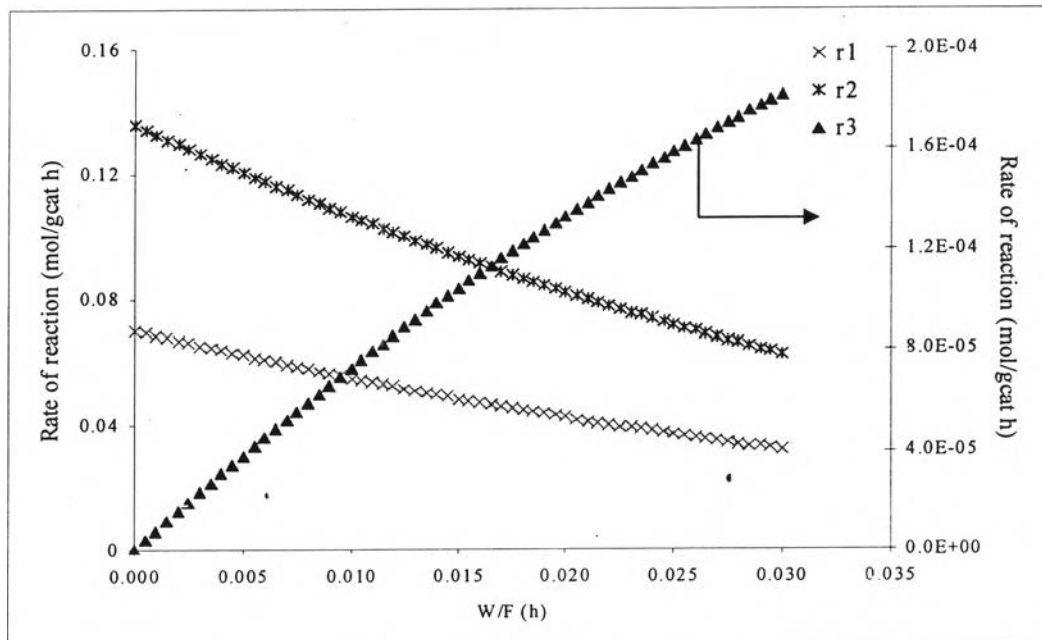


Figure 4.16 Rates of the individual reactions as a function of space times at 285 °C.

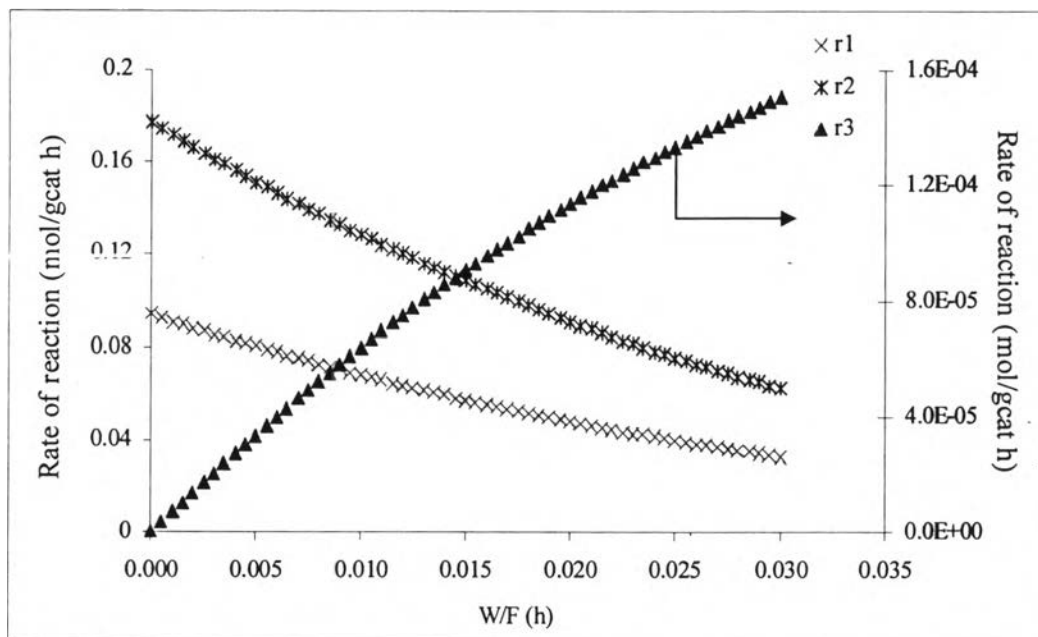


Figure 4.17 Rates of the individual reactions as a function of space times at 270 °C.

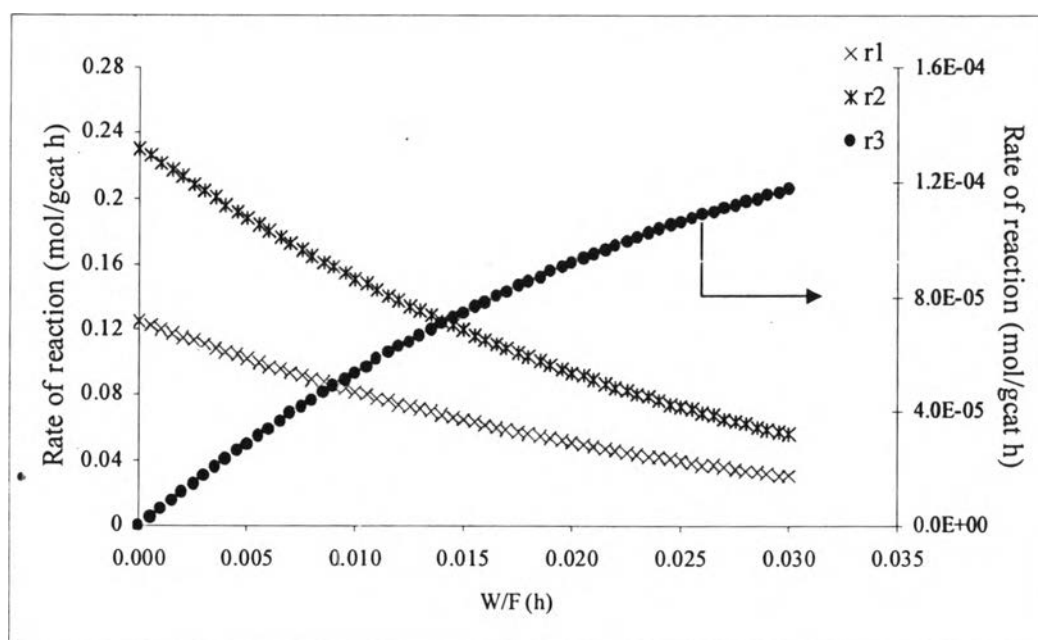


Figure 4.18 Rates of the individual reactions as a function of space times at 255 °C.



The heats of adsorption of hydrocarbons obtained from the fitting are not far from the microcalorimetry studies, in which the heat of adsorption of hydrocarbons over non-microporous surface is around 4-7 kJ/mol per carbon atom (Van Bokhoven, 2001). There are the differences between the adsorption constants of decalin isomers. Both of them have the nearly heat of adsorptions therefore the difference in entropy seems to play an important role. The largest heat of adsorption is the heat adsorption of hydrogen which is -110 kJ/mol. This value obtained from the fitting is not far from the literature. Christmann *et al.* (1974) proposed the hydrogen adsorption enthalpies of around -100 kJ/mol. Weatherbee *et al.* (1984) reported the hydrogen enthalpies of -125 kJ/mol at high temperature desorption (330 °C). Lindfors and Salmi (1993) proposed the heat of adsorption of hydrogen of 150 kJ/mol in the hydrogenation of toluene on nickel catalyst. The heat of adsorption of hydrogen was also suggested by Smed *et al.* (1996) who studied the chemisorption of hydrogen on nickel catalysts. They proposed the heat of adsorption is in the range of -110 to -120 kJ/mol. The hydrogen desorbs from the nickel surface at higher temperature can explain the decreasing in the hydrogenation rates. In addition, from the heat of adsorption obtained from the fitting, it can be shown that the hydrogen adsorption is not favor at higher temperatures. The hydrogen adsorption constant is rapidly decreased with increasing temperatures. As same as the adsorption of tetralin, heat of adsorption of tetralin is much more than *cis*- and *trans*-decalin, therefore tetralin adsorption is not favor at higher temperatures. The decreased of adsorption of hydrogen and tetralin at higher temperatures is the reason of the decreasing in the hydrogenation rates at higher temperature shown in Figures 4.19 and 4.20.

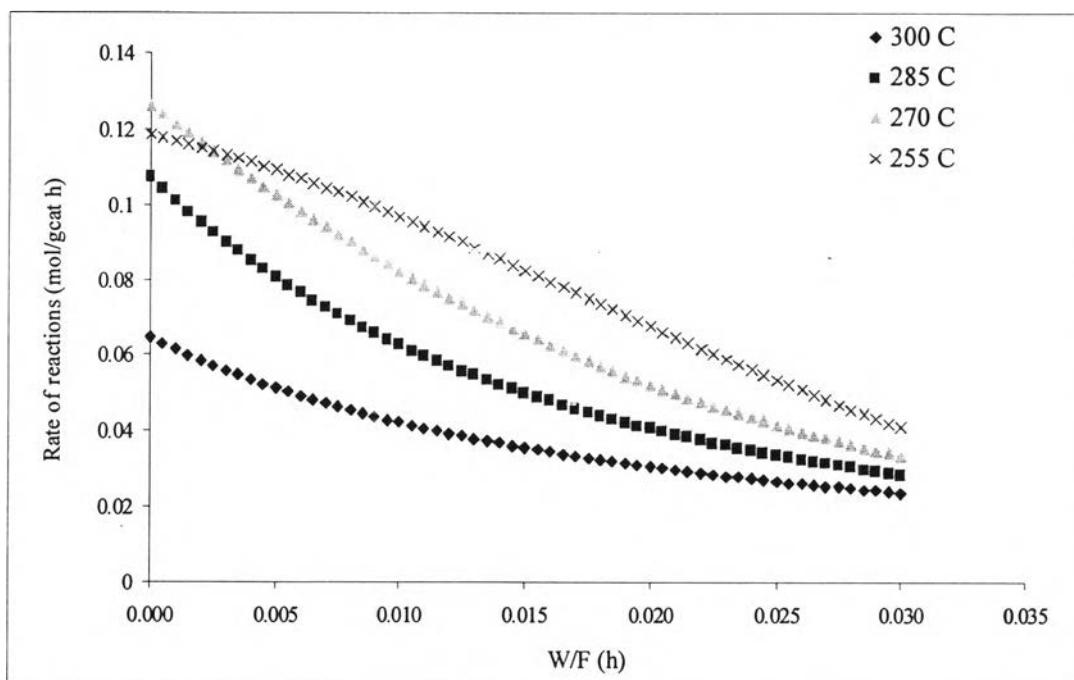


Figure 4.19 Rates of tetralin hydrogenation to *cis*-decalin at different temperatures.

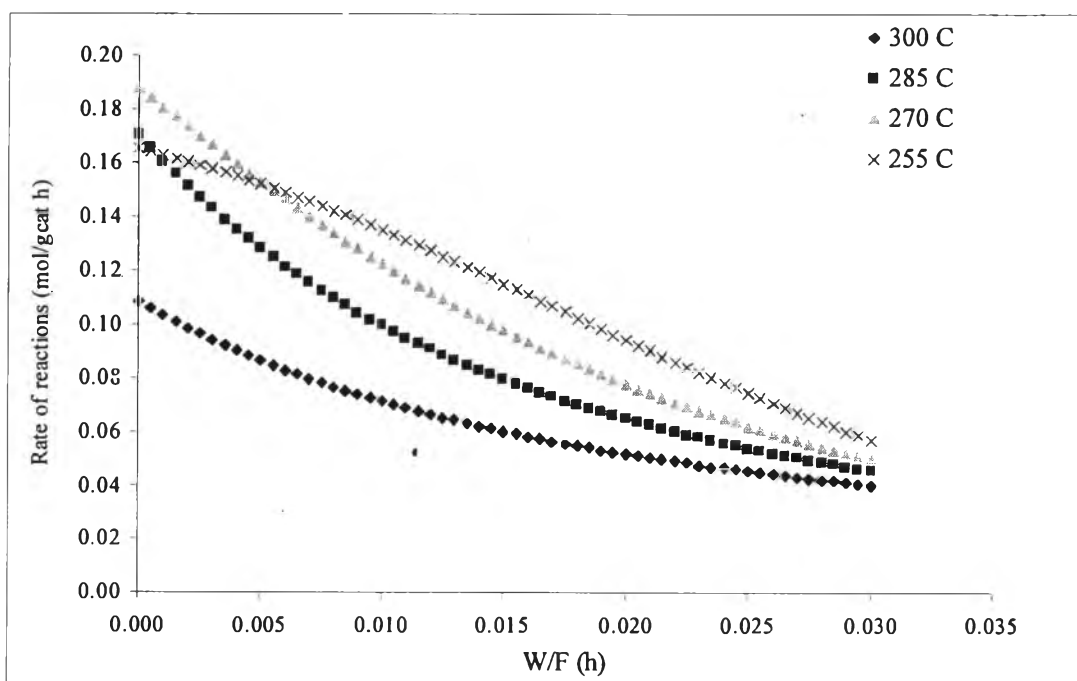


Figure 4.20 Rates of tetralin hydrogenation to *trans*-decalin at different temperatures.